Supporting Information

Supramolecular Nanofibrillar Hydrogels as Highly Stretchable, Elastic and Sensitive Ionic Sensors

Xiaohui Zhang, Nannan Sheng, Linan Wang, Yeqiang Tan, Chunzhao Liu, Yanzhi Xia, Zhihong Nie*, Kunyan Sui*

Experimental and general information

Materials.

Sodium alginate (SA) (η=460 mPa•s, 300 mPa•s) were obtained from Qingdao Hyzlin Biology Development Co., Ltd. (Qingdao Haizhilin Company, China) and it was used without further purification. Acrylamide (AM) monomer was purchased from Aladdin Chemical Co. and it was purified by passing through a short alumina column. N, N'-methylenebisacrylamide (MBAA) and N,N,N',N'-tetramethylethylenediamine (TEMED) were purchased from Aladdin Chemical Co. Sodium chloride (NaCl) (purity 99.9%), ammonium persulfate (APS) and Rhodamine B were supplied by Sinopharm Chemical Reagent, China. APS was recrystallized before use. Other reagents were used without further purification.

Preparation of the NaCl/SA/PAM DN hydrogels.

We synthesized the ionic hydrogels via one-pot free-radical polymerization.[1,2] Firstly, SA was added to different concentrations of saline solution and it was stirred at room temperature for 4 h to make SA fully swollen. Then it was stirred at constant temperature of 50 °C for 0.5 h, so that SA was fully dissolved, finally the homogeneous and stable NaCl/SA solution was obtained. The

prepared NaCl/SA solution is incubated over night at ambient temperature. AM monomer, crosslinking agent (MBAA), thermo-initiator (APS) and accelerator (TEMED) were sequentially dissolved into the above NaCl/SA solution under stirring in an ice bath, and a transparently homogeneous solution was obtained. The solution was injected into different molds to produce different shapes of DN gels and then put in an oven at 50 °C for 3 h to obtain NaCl/SA/PAM DN hydrogels. After thermo-polymerization, the obtained NaCl/SA/PAM DN hydrogels were removed from the mold and then used for mechanical and other tests.

General Characterization Techniques.

TEM was performed by a JEM-2100 instrument (JEM-2100, JEOL, Japan) operating at an accelerating voltage of 200 kV. AFM image of the SA nanofibrils was performed by using a Picoscan AFM (Molecular Imaging, Agilent Technologies) in the magnetic alternating current (MAC) mode. The rheological measurements were recorded on a rotational rheometer (MCR301, Anton Paar, Austria) with a cone-plate geometry of 25 mm in diameter and a gap of 0.05 mm. Shear recovery test of the oscillatory shear strain is increased from 1% to 3000%, angular frequency is 10 rad/s. A low-viscosity silicone oil was placed on the perimeter of the samples to prevent water evaporation during the measurements.

Mechanical Tests.

Tensile and compressive tests of the NaCl/SA/PAM DN hydrogels were performed using universal mechanical tester (WDW-5T, China) with a 250 N load cell for tension and 2000 N for compression. The samples for tension were a cylinder with a diameter of 6 mm, the tensile tests were carried out at a constant velocity of 100 mm/min at room temperature. It is noted that all the stresses measured are engineering stresses or nominal stresses which are calculated using the

following formula: $\sigma = \dfrac{F}{A_0}$, Where F is the applied load, and A_0 is the starting cross-sectional area.

The tensile strain (ε) was defined as the ratio of gauge length (L) to the initial gauge length (L_0):

$\varepsilon = \dfrac{L - L_0}{L_0}$. The elastic modulus (E) was determined by the average slope over 10−30% of strain

from the stress−strain curve by following formula: $E = \dfrac{\sigma}{\varepsilon}$. Toughness ($T$) was estimated by the area

under the stress-strain curves until fracture point by following formula: $$T = \int_{\varepsilon_0}^{\varepsilon_f} \sigma(\varepsilon)d\varepsilon$$, where ε_0

and ε_f corresponded to the initial stretch and fracture stretch, respectively. Tensile cycle tests were

carried out by performing subsequent trials immediately after the initial loading at the same

velocity of 100 mm/min. The dissipation energy was defined by the area under a cycle of

loading−unloading curve. The cylindrical samples with a height of 12 mm and a diameter of 15

mm were used for compression tests. The compressive strain was estimated as h/h_0, where h is the

height under compression and h_0 is the original height. The compressive rate was 5 mm/min.

Compression cycle tests were carried out by performing subsequent trials immediately after the

initial loading at the same velocity of 5 mm/min.

Fabrication of NaCl/SA/PAM Strain Sensors.

A strain sensor was assembled by using the NaCl/SA/PAM DN hydrogel as a conductor and VHB

tape as elastomeric substrates and encapsulant. The top and bottom of the sensor were insulated

using the VHB tape to prevent water evaporation from the hydrogel. Before the strain sensor was

assembled, the surfaces of the hydrogels were dried with N_2 gas for 30 s to improve the adhesion

between VHB and hydrogel by removing water from the hydrogel surfaces.

Characterization of NaCl/SA/PAM Strain Sensors.

The loading of tensile strain was performed with universal mechanical tester (WDW-5T, China), while the electrical signals of the strain sensors were recorded at the same time by a Keithley 2450 digital meter after the current saturated. To monitoring the human body motions, the strain sensors were attached onto different joints of the human body, such as wrist, throat, fingers, elbows and knees. The relative change of the resistance was calculated on the basis of the current monitored: $\Delta R/R_0 = (R-R_0)/R_0$, where R_0 and R are the resistance without and with applied strain, respectively. The gauge factor (GF) defined as $GF = (\Delta R/R_0)/\varepsilon$, where $\Delta R/R_0$ is the relative change in resistance and ε is the applied strain.
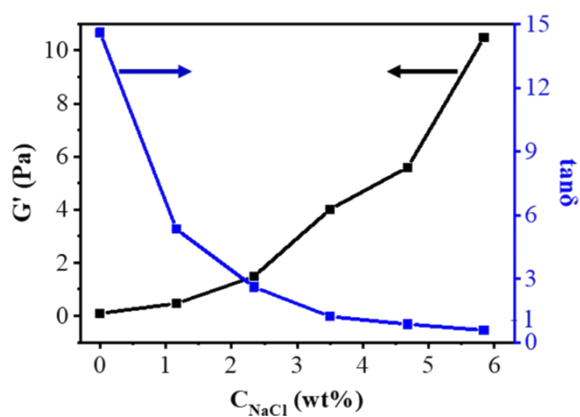
Figures

Figure S1 The storage modulus (G') and damping factor ($tan\ \delta$) of NaCl/SA solution.
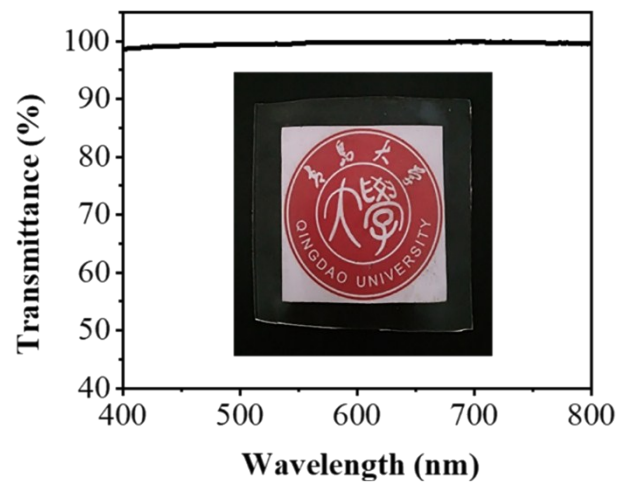
Figure S2 The transmittance of the hydrogel in the visible wavelength range of 400-800 nm.

Figure S3 The photographs of the healing process for ionic hydrogels in series-parallel as self-healable electronic interconnects with LEDs. The LEDs could work and the multimeter shows the same value of current to initial stage after the two cut pieces are pushed together at room temperature and spontaneously self-adhesive under ambient conditions without any external stimulus, indicating the good healing properties of the ionic hydrogels for electronic circuits.
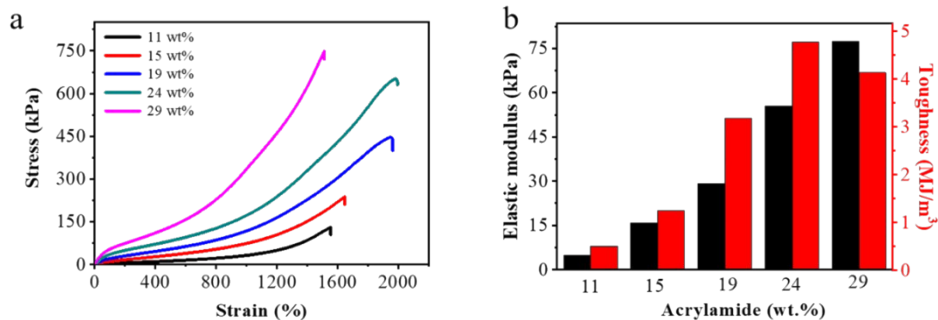
Figure S4 The concentration of AM greatly affects the behaviors of the NaCl/SA/PAM ionic hydrogels. (a) Stress-strain curves were measured with various concentrations of AM (wt%). (b) Elastic modulus and toughness of the gels.
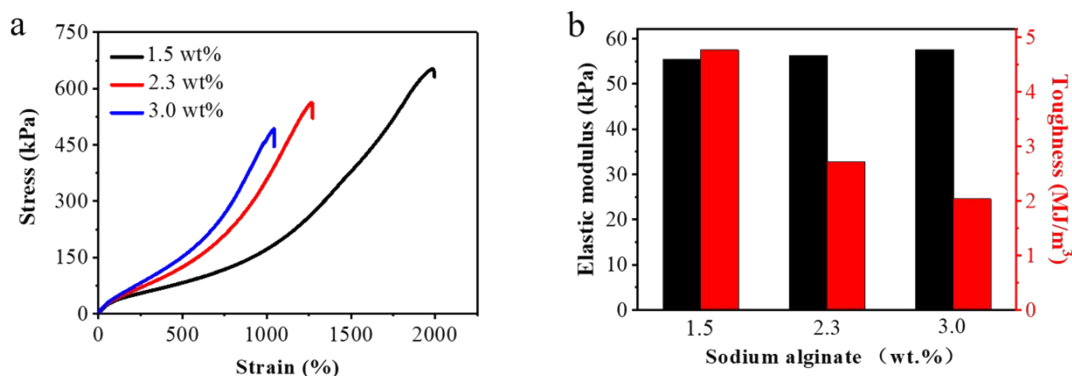

Figure S5 The concentration of SA greatly affects the behaviors of the hybrid supramolecular ionic hydrogels. (a) Stress-strain curves were measured with various concentrations of SA (wt%). (b) Elastic modulus and toughness of the gels.
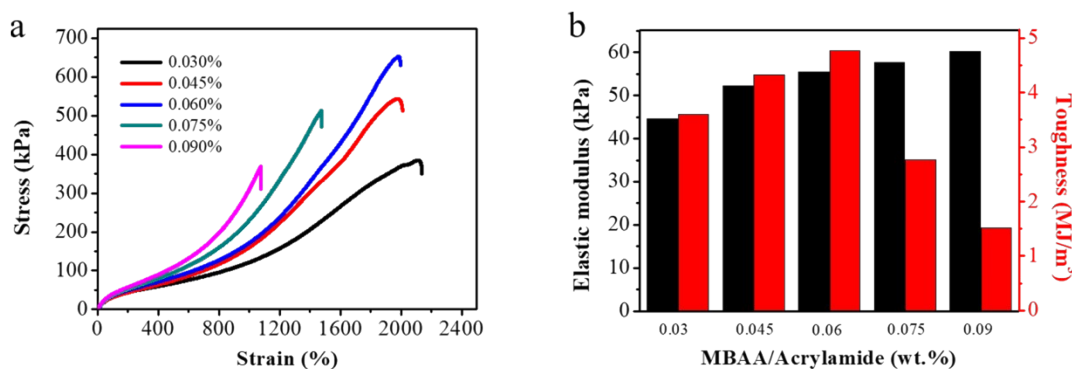
Figure S6 The amount of covalent crosslinker, MBAA, greatly affects the behaviors of the hybrid supramolecular ionic hydrogels. (a) Stress-strain curves were measured with various concentrations of MBAA (wt%). (b) Elastic modulus and toughness of the gels.
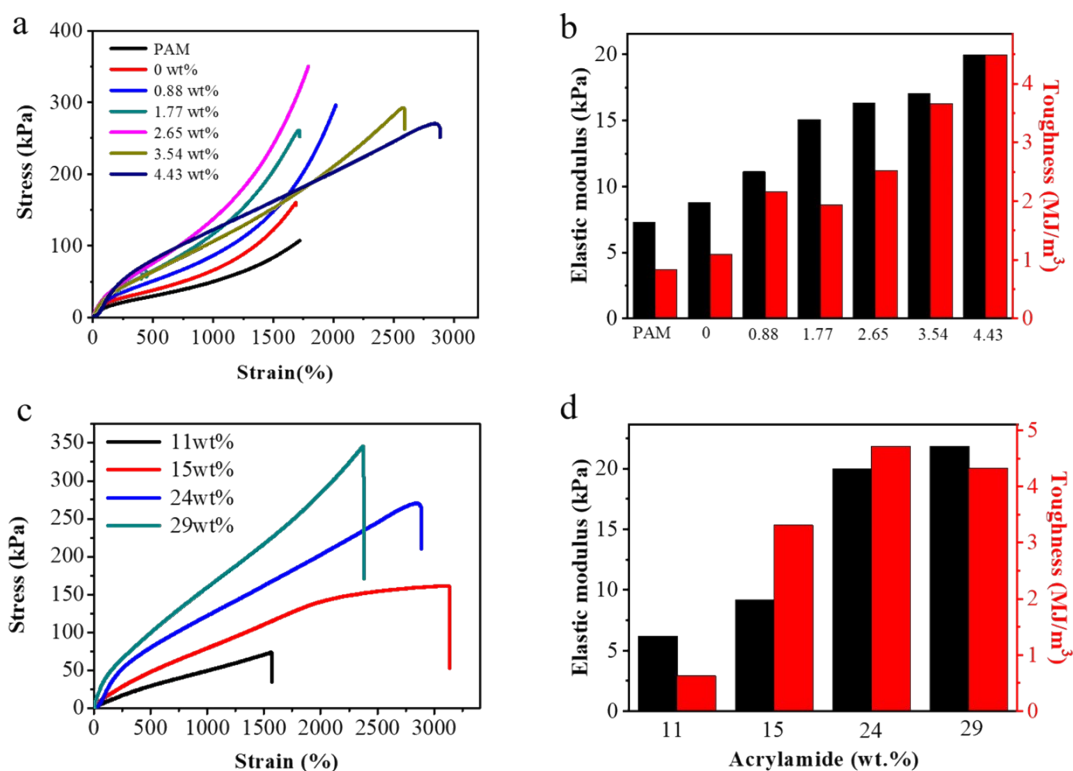
Figure S7 The molecular weight of SA greatly affects the behaviors of the NaCl/SA/PAM supramolecular ionic hydrogels. In this system, we use low molecular weight (LMW) SA (η= 300 mPa•s) instead of high molecular weight (HMW) SA (η= 460 mPa•s). (a) Tensile stress of PAM and NaCl/SA/PAM gels with different C_{NaCl} at fixed concentration of SA (1.5 wt%, 300 mPa•s), AM (24 wt%), MBAA =0.06 wt%. (b) Toughness and elastic modulus of PAM and NaCl/SA/PAM gels with different C_{NaCl}. (c) Stress-strain curves were measured with various values of AM (wt%). (d) Elastic modulus and toughness of the hybrid gels.

It can be seen that the strength and stretchability of NaCl/SA/PAM are also much higher than that of parent hydrogels by using LMW SA. However, the strength of the DN hydrogels by using LMW SA is ~300 kPa lower than that of HMW ones, while the stretchability is higher than that of HMW, reaching maximum uniaxial tensile strain more than 3000%, which is demonstrated in Figure S7 (a, c).

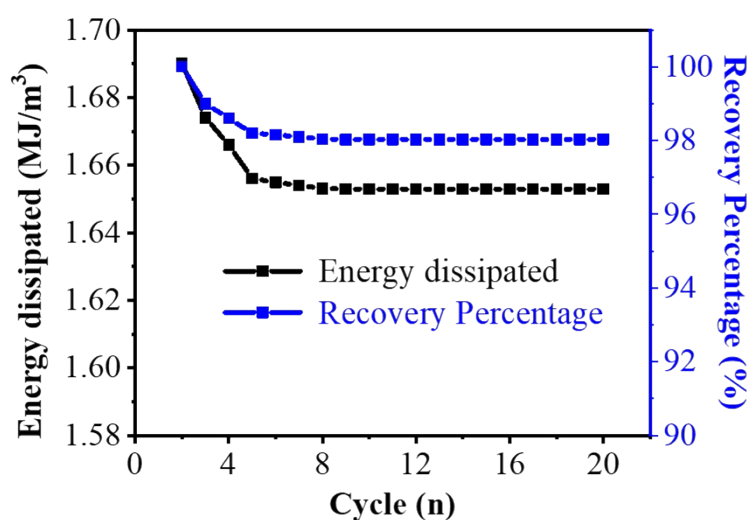**Figure S8** The energy dissipated (black) and recovery percentage (blue) of the gels in 20 continuous tension-relaxation cycles shown in Figure 2c.
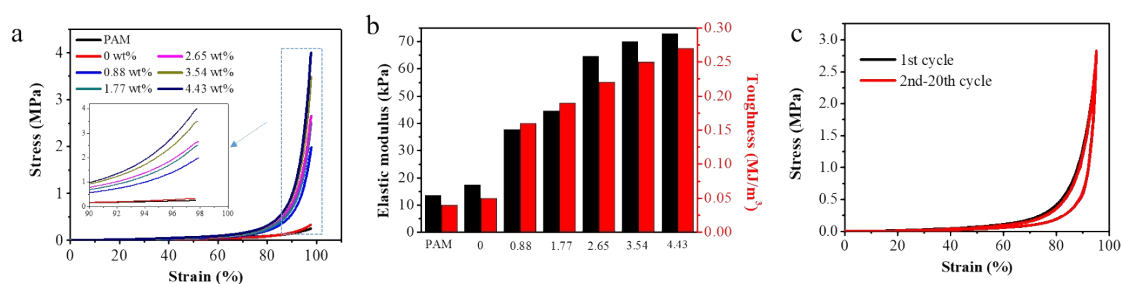
Figure S9 Compression mechanical properties of NaCl/SA/PAM ionic hydrogels. (a) stress-strain curves of gels with different C_{NaCl} at fixed concentration of SA (1.5 wt%), AM (24 wt%), MBAA (0.06 wt%, mass percent concentration to AM). Toughness and modulus (b) calculated from

stress–strain curves of gels as a function of C_{NaCl}. The relaxation cycles to the same

NaCl/SA/PAM gel for 20 cycles under a compression of 98% (c).

Figure S10 When compressed with 98% of their original heights, the PAM gel was fractured

completely, while SA/PAM gel could not be restored to its original state though without fracture.

In contrast, NaCl/SA/PAM hydrogel recovered to its original shape immediately after release of

the loading even at 98% strain.

Figure S11 Experimental data and theoretical prediction of capacitance as a function of stretch

when our ionic hydrogels are used as capacity-type sensor.

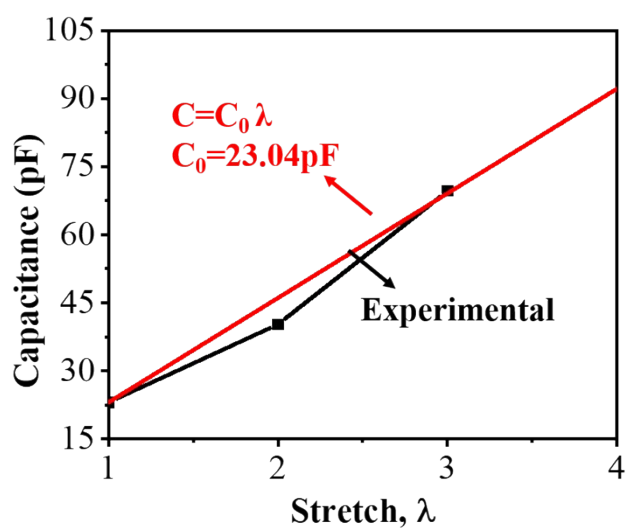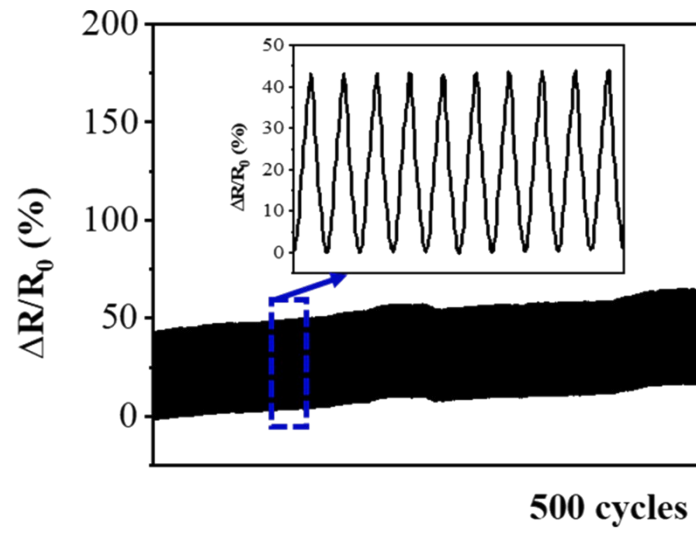**Figure S12** Relative change in resistance under cyclic loading of 50% strain for 500 cycles,

showing the high stability of the sensor.

Table S1. Comparisons of the tough DN hydrogels

Composition	Tension			Compression			Recovery	Injectable	Reference
	σ [MPa]	ε [λ]	E [kPa]	σ [MPa]	ε [%]	E [kPa]	[%] (Time, T)		
NaCl/SA/PAM	**0.65**	**20**	**50**	**No fracture**	**Anti-car crash**	**45**	**100% (instantly, R.T.)**	**√**	**This work**
Ca^{2+}/SA/PAM	0.156	23	29	/[1]	/	/	74% (1 day, 80 ℃)	/	[1]
Ca^{2+}/SA/PAM	0.25	17	100	/	/	/	/	/	[3]
Fe^{3+}/SA/PAM	0.943	14	252.2	/	/	/	/	/	[4]
Ca^{2+}/SA/PEGDA	0.25	4.5	/	/	/	/	70.5% (24 h, 37 ℃)	√	[5]
Chitin/ECH/EtOH	/	/	/	3.98	81	220	poor	/	[6]
Chitosan /ECH/ EtOH	0.37	1.17	200	4.83	77.7	430	/	/	[7]
Chitosan/PAM/NaOH	1.94	5	357.6		Anti-car crash		90% (4 h)	/	[8]
Cellulose/ECH/EtOH	2.7	0.81	2000	4.8	74	610	/	/	[9]
Fe^{3+}/p(AAm-co-AAc)	5.9	7.48	1800	/	/	/	87.6% (4 h)	/	[10]
Agar/PAM	1	20	/	38	98	123	65% (10 min, 100 ℃)	/	[11]
Agar/pHEAA	2.6	8	2400	35	/	/	62% (120 min, 95℃)	/	[12]
Agar/HPAM	0.267	52.6	106	/	/	/	40% (2 min)	/	[13]
Peptide/PAM	/	/	/	0.21	66.38	329	90% (instantly)	/	[14]
DMAA/MAAc	2	4.5	28000	/	/	/	100% (3min, 37 ℃)	/	[15]
Host-guest CB-8/PAM	0.13	20	35	/	/	/	100% (30 min)	/	[16]
PVP/PAM	1.2	30	84	17	95	/	/	/	[17]
Gelatin/(NH$_4$)$_2$SO$_4$	4.307	4.2	758.2	>13.01	>99	458	/	/	[18]
BSICT/SF	0.56	1.3	2600	1.6	70	/	61% (1h)	/	[19]
HPMC/ RSF	0.37	1.2	1230	/	/	1450	/	/	[20]

Note: '/' indicates 'not shown' in the references.

Table S2.   Resistance of NaCl/SA/PAM hydrogels.

SA (wt%)	PAM (wt%)	NaCl (wt%)	Resistance (MΩ)	Conductivity $\sigma*10^2$ (S/m)
1.5	24	0	1.41	0.36
1.5	24	0.88	0.55	0.93
1.5	24	1.77	0.22	2.32
1.5	24	2.65	0.38	1.34
1.5	24	3.54	0.14	3.64
1.5	24	4.43	0.09	5.66

Table S3. Comparisons of some E-skins

Type	Component	Tension σ [kPa]	Tension ε [λ]	Compression σ [MPa]	Sensitivity [kPa⁻¹]	Gauge factor	Injectable	Detection Limit Strain [%]	Detection Limit Pressure [Pa]	Operating voltage [V]	Ref.
I [a]	NaCl/SA/PAM	650	20	No fracture	1.45	2.66	√	0.3-1800	100	0.04-0.5	This work
I	PAM/NaCl	/	6	/	/	/	/	1-500	1000	1	[21]
I	PAM/LiCl	27	11	/	/	/	/	/	/	1	[22]
I	PAM/LiCl/PDMS	/	0.5	/	/	0.84	√	40	/	/	[23]
I	KCl/κ-Carrageenan/PAM	575	20	/	/	0.63	√	1000	/	5	[2]
I	NaCl/AA/DMAPS	2000	100	0.05	/	/	/	100	/	/	[24]
I	ACC/PAA/SA	5	10	0.004	0.17	/	/	/	/	1	[25]
I	PVDF-co-HFP/EMIOTf	2	54	/	/	/	/	/	/	/	[26]
I	PAMPS/[EMIm][DCA]	400	1.6	7.7	/	/	/	/	/	/	[27]
I	AA/AETA/SiO$_2$	6	3.7	/	/	/	√	/	/	0.05	[28]
I	Fe^{3+}/AA/DCh-PPy	7	15	0.06	/	/	√	/	/	/	[29]
E [b]	SWNTs/PDMS	/	/	/	1.80	/	/	/	0.6	2	[30]
E	Ag(Au)NWs/PDMS	/	0.7	/	/	5	/	0.05-70	/	0.1	[31]
E	SWNT/PVA	/	10	/	/	1.51	/	2-1000	/	5	[32]
E	SWCNT/PDMS	/	2.8	/	/	0.06	/	2-280	/	/	[33]
E	CNT/PDMS	/	1.7	/	/	0.41	/	170	/	/	[34]
E	CSFs/Ecoflex	/	5	/	/	37.5	/	2-500	/	3	[35]
E	Graphene/Silly Putty	300	0.5	/	/	535	/	/	/	1	[36]
E	ACNT/G/PDMS	/	/	/	19.80	/	/	/	0.6	0.03	[37]
E	Pt/PUA/ PDMS	/	/	/	/	11.45	/	5	5	/	[38]

Note: '/' indicates 'not shown' in the references.

[a,b] 'I' and 'E' means 'ionic conductor' and 'electronic conductor', respectively;

Movie S1. The compression experiment for NaCl/SA/PAM gel.

Movie S2. Undergoing repeating car crash experiment for NaCl/SA/PAM gel.

13

Movie S3. Undergoing repeating car crash experiment for SA/PAM gel.

Movie S4. Undergoing repeating car crash experiment for PAM gel.

Movie S5. The video of quickly stretch and release the hydrogel with large strain. The result shows that the ionic hydrogel have excellent elasticity, stability, and fast response.

Movie S6. The video of relative resistance changes versus time for monitoring the finger bending in real time. It can be seen that the variation of the resistance is completely synchronous with the motion of finger bending for many times and could minor jitter of the finger with high sensitivity.

References

[1] J. Y. Sun, X. H. Zhao, W. R. K. Illeperuma, O. Chaudhuri, K. H. Oh, D. J. Mooney, J. J. Vlassak and Z. G. Suo, *Nature*, 2012, **489**, 133-136.

[2]   S. J. Liu and L. Li, *ACS Appl. Mater. Interfaces*, 2017, **9**, 26429-26437.

[3]   J. Y. Li, W. R. K. Illeperuma, Z. G. Suo and J. J. Vlassak, *ACS Macro. Lett.*, 2014, **3**, 520-523.

[4]   C. H. Yang, M. X. Wang, H. Haider, J. H. Yang, J. Y. Sun, Y. M. Chen, J. X. Zhou and Z. G.Suo, *ACS Appl. Mater. Interfaces*, 2013, **5**, 10418-10422.

[5] S. Hong, D. Sycks, H. F. Chan, S. T. Lin, G. P. Lopez, F. Guilak, K. W. Leong and X. H. Zhao, *Adv. Mater.*, 2015, **27**, 4035-4040.

[6] D. D. Xu, J. C. Huang, D. Zhao, B. B. Ding, L. N. Zhang and J. Cai, *Adv. Mater.*, 2016, **28**, 5844-5849.

[7] J. J. Duan, X. C. Liang, Y. Cao, S. Wang and L. N. Zhang, *Macromolecules*, 2015, **48**, 2706-2714.

[8]   Y. Y. Yang, X. Wang, F. Yang, H. Shen and D. C. Wu, *Adv. Mater.*, 2016, **28**, 7178-7184.

[9]   D. Zhao, J. C. Huang, Y. Zhong, K. Li, L. N. Zhang and J. Cai, *Adv. Funct. Mater.*, 2016,

26, 6279-6287.

[10]   P. Lin, S. H. Ma, X. L. Wang and F. Zhou, *Adv. Mater.*, 2015, **27**, 2054-2059.

[11]   Q. Chen, L. Zhu, C. Zhao, Q. M. Wang and J. Zheng, *Adv. Mater.*, 2013, **25**, 4171-4176.

[12] H. Chen, Y. L. Liu, B. P. Ren, Y. X. Zhang, J. Ma, L. J. Xu, Q. Chen and J. Zheng, *Adv. Funct. Mater.*, 2017, **27**, 1703086.

[13] Q. Chen, L. Zhu, H. Chen, H. L. Yan, L. N. Huang, J. Yang and J. Zheng, *Adv. Funct. Mater.*, 2015, **25**, 1598-1607.

[14] W. X. Sun, B. Xue, Y. Li, M. Qin, J. Y. Wu, K. Lu, J. H. Wu, Y. Cao, Q. Jiang and W. Wang, *Adv. Funct. Mater.*, 2016, **26**, 9044-9052.

[15] X. B. Hu, M. V. Varnoosfaderani, J. Zhou, Q. X. Li and S. S. Sheiko, *Adv. Mater.*, 2015, **27**, 6899-6905.

[16] J. Liu, C. S. Y. Tan, Z. Y. Yu, Y. Lan, C. Abell and O. A. Scherman, *Adv. Mater.*, 2017, **29**, 1604951.

[17] G. S. Song, L. Zhang, C. C. He, D. C. Fang, P. G. Whitten and H. L. Wang, *Macromolecules*, 2013, **46**, 7423-7435.

[18] Q. Y. He, Y. Huang and S. Y. Wang. *Adv. Funct. Mater.*, 2018, **28**, 1705069.

[19] Z. H. Zhu, S. J. Ling, J. J. Yeo, S. W. Zhao, L. Tozzi, M. J. Buehler, F. Omenetto, C. M. Li and D. L. Kaplan, *Adv. Funct. Mater.*, 2018, **28**, 1704757.

[20] K. Y. Luo, Y. H. Yang and Z. Z. Shao, *Adv. Funct. Mater.*, 2016, **26**, 872-880.

[21] J. Y. Sun, C. Keplinger, G. M. Whitesides and Z. G. Suo, *Adv. Mater.*, 2014, **26**, 7608-7614.

[22] C. C. Kim, H. H. Lee, K. H. Oh and J. Y. Sun, *Science*, 2016, **353**, 682-687.

[23] K. Tian, J. Bae, S. E. Bakarich, C. H. Yang, R. D. Gately, G. M. Spinks, M. Panhuis , Z. G. Suo and J. J. Vlassak, *Adv. Mater.*, 2017, **29**, 1604827.

[24] Z. Y. Lei and P. Y. Wu, *Nat. Commun.*, 2018, **9**, 1134.

[25] Z. Y. Lei, Q. K. Wang, S. T. Sun, W. C. Zhu and P. Y. Wu, *Adv. Mater.*, 2017, **29**, 1700321.

[26] Y. Cao, T. G. Morrissey, E. Acome, S. I. Allec, B. M. Wong, C. Keplinger and C. Wang, *Adv. Mater.*, 2017, **29**, 1605099.

[27] Y. Ding, J. J. Zhang, L. Chang, X. Q. Zhang, H. L. Liu and L. Jiang, *Adv. Mater.*, 2017, **29**, 1704253.

[28] J. Odent, T. J. Wallin, W. Y. Pan, K. Kruemplestaedter, R. F. Shepherd and E. P. Giannelis,

Adv. Funct. Mater., 2017, **27**, 1701807.

[29]   M. A. Darabi, A. Khosrozadeh, R. Mbeleck, Y. Q. Liu, Q. Chang, J. Z. Jiang, J. Cai, Q. Wang, G. X. Luo and M. Xing, *Adv. Mater.*, 2017, **29**, 1700533.

[30]   X. W. Wang, Y. Gu, Z. P. Xiong, Z. Cui and T. Zhang, *Adv. Mater.*, 2014, **26**, 1336-1342.

[31]   M. D. Ho, Y. Z. Ling, L. W. Yap, Y. Wang, D. S. Dong, Y. M. Zhao and W. L. Cheng, *Adv. Funct. Mater.*, 2017, **27**, 1700845.

[32]   G. F. Cai, J. X. Wang, K. Qian, J. W. Chen, S. H. Li and P. S. Lee, *Adv. Sci.*, 2017, **4**, 1600190.

[33]   T. Yamada, Y. Hayamizu, Y. Yamamoto, Y. Yomogida, A. I. Najafabadi, D. N. Futaba and K. Hata, *Nat. Nanotechnol.*, 2011, **6**, 296-301.

[34]   D. J. Lipomi, M. Vosgueritchian, B. C. K. Tee, S. L. Hellstrom, J. A. Lee, C. H. Fox and Z. N. Bao, *Nat. Nanotechnol.*, 2011, **6**, 788-792.

[35]   C. Y. Wang, X. Li, E. L. Gao, M. Q. Jian, K. L. Xia, Q. Wang, Z. P. Xu, T. L. Ren and Y. Y. Zhang, *Adv. Mater.*, 2016, **28**, 6640-6648.

[36]   C. S. Boland, U. Khan, G. Ryan, S. Barwich, R. Charifou, A. Harvey, C. Backes, Z. L. Li, M. S. Ferreira, M. E. Möbius, R. J. Young and J. N. Coleman, *Science*, 2016, **354**, 1257-1260.

[37]   M. Q. Jian, K. L. Xia, Q. Wang, Z. Yin, H. M. Wang, C. Y. Wang, H. H. Xie, M. C. Zhang and Y. Y. Zhang, *Adv. Funct. Mater.*, 2017, **27**, 1606066.

[38]   C. Pang, G. Y. Lee, T. I. Kim, S. M. Kim, H. N. Kim, S. H. Ahn and K. Y. Suh, *Nat. Mater.*, 2012, **11**, 795-801.